·Experimental Research·

Therapeutic effect of anti-IL-12/IL-23 p40 on experimental autoimmune uveitis and associated mechanism

Cui Xuexue, Zhang Zhihui, Wu Lingzi, Li Yongtao, Chen Shuang, Chen Nu, Zhang Xiaomin

Tianjin Key Laboratory of Retinal Functions and Diseases, Tianjin Branch of National Clinical Research Center for Ocular Disease, Eye Institute and School of Optometry, Tianjin Medical University Eye Hospital，Tianjin 300384, China

Corresponding author: Zhang Xiaomin, Email: xzhang08@tmu.edu.cn

[Abstract]

Objective To explore the therapeutic effect of anti-interleukin(IL)-12/IL-23 p40 antibodies on experimental autoimmune uveitis (EAU) and its associated mechanism.

Methods Sixty-six SPF female C57BL/6N mice aged 6-8 weeks were selected. An EAU model was established in 24 mice via immunization with the interphotoreceptor retinoid-binding protein (IRBP) 651-670. The 24 mice were sacrificed before immunization, and on days 3, 12, and 18 post-immunization (6 mice/time point). Flow cytometry was used to detect the proportion of IL-17A$^+$ interferon-γ (IFN-γ)$^+$ CD4$^+$ T cells in the spleen, lymph nodes, and eyeballs. Another 6 mice were selected to establish the EAU model, and fundus images of the mice were obtained using a small animal imaging instrument and optical coherence tomography (OCT) on day 18 post-immunization. The mice were sacrificed after OCT examination and the eyeballs were collected. Hematoxylin-eosin staining was used to observe retinal inflammation and morphological changes in the tissue structure. Flow cytometry was employed to detect the proportion of IL-17A$^+$ IFN-γ$^+$ CD4$^+$ T cells in lymph nodes. The 6 mice were divided into IL-17A$^+$ IFN-γ$^+$ high expression group and IL-17A$^+$ IFN-γ$^+$ low expression group according to the flow cytometry results, and the degree of retinal injury was compared between the two groups. An EAU model was established in another 36 mice, which were divided into anti-IL-12/IL-23 p40 group and IgG group using the random number table method (18 mice/group). Anti-IL-12/IL-23 p40 or IgG was injected by tail vein at 3-day intervals according to grouping. On days 12 and 18 post-immunization, 6 mice were selected from each group to collect lymph nodes and eyeballs. The proportion of T cell subsets was detected by flow cytometry. Eyeballs of 6 mice in each group were extracted on day 24 post-immunization and retinal damage was observed by hematoxylin-eosin staining. The induced differentiation of CD4$^+$ T cells *in vitro* was assayed by flow cytometry. The IL-17 and IFN-γ expression was detected by enzyme-linked immunosorbent assay (ELISA) after the induced differentiation of IL-17A$^+$ IFN-γ$^+$ CD4$^+$ T cells. The relative levels of Th1 transcription factor T-bet and Th17 transcription factor retinoid acid-related orphan nuclear receptor γt (ROR-γt) expression after the induced differentiation of IL-17A$^+$ IFN-γ$^+$ CD4$^+$ T cells were detected by real-time quantitative PCR. The use and care of animals was in accordance with the ARVO statement and this study protocol was approved by an Ethics Committee of Experimental Animals of Tianjin Medical University Eye Hospital (No. TJYY2019111019).

Results Significant differences were observed regarding the proportion of IL-17A$^+$ IFN-γ$^+$ CD4$^+$ T cells in lymph nodes, spleen, and eyeballs between the wild-type and EAU mice on days 3, 12, and 18 post-immunization (H = 9.642, 16.531, 10.385; all at $P < 0.05$). Compared with pre-immunization levels, the proportion of IL-17A$^+$ IFN-γ$^+$ CD4$^+$ T cells was significantly increased in the lymph nodes of EAU mice on day 12 post-immunization and was significantly increased in spleen and lymph nodes on day 18 post-immunization (all at $P < 0.05$). Severe retinal exudation, retinal detachment, severe inflammatory cell infiltration and extensive retinal folds were detected in IL-17A$^+$ IFN-γ$^+$ high expression mice. Mild retinal edema, focal inflammatory cell infiltration and mild retinal folds were observed in IL-17A$^+$ IFN-γ$^+$ low expression mice. The proportion of CD3 and IL-17A$^+$ IFN-γ$^+$ CD4$^+$ T cells in the eyeballs of the anti-IL-12/IL-23 p40 group was significantly lower than that in the IgG group on day 18 post-immunization (t=15.304, 8.080; both at $P < 0.05$). On day 12 post-immunization, the percentage of IL-17A$^+$ IFN-γ$^+$ CD4$^+$ T cells in anti-IL-12/IL-23 p40 group was 0.33 ± 0.18%, which was significantly lower than 4.83 ± 0.45% in the IgG group (t=15.974, $P < 0.001$). Compared with IgG group, the percentage of Th1, Th17, IL-17A$^+$ IFN-γ$^+$ CD4$^+$ T cells and the level of IL-17, IFN-γ, T-bet, and ROR-γt expression in the anti-IL-12/IL-23 p40 treatment group were significantly decreased (all at $P < 0.05$).

Conclusions Anti-IL-12/IL-23 p40 treatment has a therapeutic effect on EAU by inhibiting IL-17A$^+$ IFN-γ$^+$ CD4$^+$T cells.

Keywords Uveitis; Drug therapy; Interleukin-12 subunit p40; Monoclonal antibodies; Interphotoreceptor retinoid-binding protein; Mice

Fund program: National Natural Science Foundation of China (81671642, 82171042, and 81870651); Key Project of Tianjin Science and Technology Support (20YFZCSY00990); Key Project of Natural Science Foundation of Tianjin (20JCZDJC00100); Tianjin Medical Key Discipline (Specialty) Construction Project (TJYXZDXK-037A)

DOI: 10.3760/cma.j.cn115989-20200820-00601

Autoimmune uveitis is a serious vision-threatening inflammatory disease, the pathogenesis of which is complex and unclear. The intraocular inflammatory response caused by CD4$^+$ T cell dysfunction has been found to play a pivotal role in the development of uveitis. Moreover, the presence of interleukin (IL)-17A$^+$ interferon-γ (IFN-γ)$^+$ CD4$^+$ T cells was observed in tissue-specific inflammation sites of both humans and mice. IL-17A$^+$ IFN-γ$^+$ CD4$^+$ T cells are characterized by low cytotoxicity, high pathogenicity, and low sensitivity to regulatory T cells (Tregs) [1]. Thus, this T cell subset has become a new therapeutic target for various autoimmune diseases, including inflammatory bowel disease (IBD), multiple sclerosis, rheumatoid arthritis, and recurrent uveitis [2-5]. The formation of IL-17A$^+$ IFN-γ$^+$ CD4$^+$ T cells is a complex process that involves the interaction between multiple cytokines; in particular, IL-12 and IL-23 are known to play a key role [6-7]. IL-12 (heterodimer of p35 and p40) and IL-23 (heterodimer of p19 and p40) share a common p40 subunit. Therefore, monoclonal antibodies directed against the p40 subunit can inhibit both IL-12R and IL-23R signal transduction [8-9]. In addition, anti-IL-12/IL-23 p40 monoclonal antibodies have been used clinically to treat chronic inflammatory diseases, such as psoriasis, psoriatic arthritis and Crohn's disease, exhibiting remarkable efficacy [10-13]. However, the role of anti-IL-12/IL-23 p40 antibody treatment in patients with autoimmune uveitis and animal model experimental autoimmune uveitis (EAU) remains unclear. In this study, we aims to explore the dynamic changes of IL-17A$^+$ IFN-γ$^+$ CD4$^+$ T cells in the

pathogenesis of EAU, as well as the therapeutic effect and mechanism of anti-IL-12/IL-23 p40 antibodies on EAU.

1 Materials and Methods

1.1 Materials

1.1.1 Mice Sixty-six healthy female SPF-grade C57BL/6 mice, 6-8 weeks of age were purchased from Beijing Weitong Lihua Experimental Animal Technology Co., Ltd. (Animal License No. SCXK [Beijing] 2016-0006). All animals were maintained in the animal facility at Tianjin Medical University Eye Hospital, at a room temperature of 23°C ± 2°C, relative humidity of 50%-60%, light intensity not exceeding 300 lx, and a 12-hour day-night cycle. All animal procedures adhered to the Association for Research in Vision and Ophthalmology (ARVO) statement formulated by the American Association for Vision and Ophthalmology Research. This research protocol was approved by the Experimental Animal Ethics Committee of Tianjin Medical University Eye Hospital (Approval number: TJYY2019111019).

1.1.2 Instruments and reagents Interphotoreceptor retinoid-binding protein peptide (IRBP) 651-670 (Shanghai Bioengineering Co., Ltd.); Complete Freund's adjuvant (Sigma, USA); Pertussis Toxin (List Labs, USA); CD4 Cell Isolation Kit (Invitrogen Life Technology Co., Ltd., USA); Anti-mouse IL-12/IL-23 p40 monoclonal antibody (16712381, Thermo Fisher, USA); Rat IgG (Thermo Fisher Scientific, Shanghai, China); Brefeldin A, Ionomycin (Med Chem Express Inc., USA); Phorbol 12-myristate 13-acetate (PMA) (Abcam, UK); anti-mouse APC-CD4 monoclonal antibody (100412), anti-mouse PE-IL-17A monoclonal antibody (506903), anti-mouse FITC-IFN-γ monoclonal antibody (505806), anti-mouse Brilliant Violet 421™-CD3 monoclonal antibody (100228) (Biolegend, USA); Small animal imager (Pleasanton, USA); flow cytometer (BD, USA); and PCR instrument (Life Technologies, USA) were used in this study.

1.2 Methods

1.2.1 Induction of EAU Human IRBP 651-670 (250 μg/mouse) and complete Freund's adjuvant emulsion (200 μL/mouse) were subcutaneously injected into the footpad, tail base, and trunk of mice as previously described [14]. Prior to immunization and 24 h post-immunization, mice were intraperitoneally injected with pertussis toxin (0.5μg/mice) as an additional immune adjuvant.

1.2.2 Flow cytometry detection of IL-17A$^+$ IFN-γ$^+$ CD4$^+$ T cells Twenty-four mice were selected and sacrificed by intraperitoneal injection of an overdose of 4% chloral hydrate on days 3, 12, and 18 post-immunization (six mice/ time point). The spleen and lymph nodes were prepared into a single-cell suspension, and red blood cells were lysed with red blood cell lysis solution for 5 min. Cell lysates were cleared by washing twice with phosphate buffered saline (PBS). Eyes were enucleated, the lenses were removed, the eyecups were cut into pieces, ground, and digested with 1 mg/mL collagenase D. The samples were incubated at 37°C for 1 h on a shaker, and the obtained cells were washed twice with PBS. Cells were resuspended in complete medium (RPMI 1640/10% FBS) and seeded into 96-well plates at a concentration of 1 × 10^6 cells/mL. The cells were stimulated with phorbol myristate acetate, ionomycin, and Brefeldin A for 5 h at 37°C. The cells were collected in a flow tube, treated with 2 μL APC-CD4 monoclonal antibody and incubated at 4°C for 30 min in the dark. The cells were washed three times with PBS, and 2 mL cell permeation solution was added to disrupt the membrane. A mixture of 2 μL PE-IL-17A monoclonal antibody and 2 μL FITC-IFN-γ monoclonal antibody were added and incubated at 4°C for 30 min in the dark. The cells were washed three times with PBS and detected by flow cytometry. The cells were determined using the forward and side scatter. IL-17A$^+$ IFN-γ$^+$ CD4$^+$ T cells were gated according to CD4, IL-17A, and IFN-γ expression.

1.2.3 OCT instrument and small animal imager To detect the retinopathy of mice in IL-17A$^+$ IFN-γ$^+$ high expression group and IL-17A$^+$ IFN-γ$^+$ low expression group, at 18 days post-immunization, 6 mice were subjected to general anesthetic. Frequency domain optical coherence tomography (OCT) was used to scan the mouse fundus centered on the optic disc to observe retinal edema, inflammatory cell leakage, and retinal detachment. A small animal imager was used to collect conventional visible light fundus images and observe the chorioretinal inflammatory infiltration, occurrence of subretinal vitreous hemorrhage,and retinal detachment. After these observations, the mice were sacrificed and the lymph nodes were removed. The frequency of IL-17A$^+$ IFN-γ$^+$ CD4$^+$ T cells in the lymph node tissues were analyzed by flow cytometry. Six mice were divided into IL-17A$^+$ IFN-γ$^+$ high expression group and IL-17A$^+$ IFN-γ$^+$ low expression group according to the flow cytometry results, and the degree of retinal injury was compared between the two groups.

1.2.4 Hematoxylin-eosin staining The morphological changes in the retina of the IL-17A$^+$ IFN-γ$^+$ high expression group and IL-17A$^+$ IFN-γ$^+$ low expression group were observed by hematoxylin-eosin staining. The eyeballs were collected from the mice and fixed in 10% formaldehyde/PBS for 24 h. The tissues were embedded in paraffin, and 5-μm-thick tissue sections were obtained from around the optic nerve region. Hematoxylin-eosin staining was performed to observe the infiltration of inflammatory cells in various layers of the retina or vitreous cavity, retinal folds, retinal detachments, and the presence of subretinal neovascularization.

1.2.5 Injection of anti-IL-12/IL-23 p40 antibodies via tail vein in EAU mice A total of 36 mice were randomly divided into either an anti-IL-12/IL-23 p40 group or IgG group using the random number table method (18 mice/group). From day 0 post-immunization, anti-IL-12/IL-23 p40 or IgG antibodies were injected via the tail vein at a three-day interval according to the group (all 500 □ g/mice). On days 12 and 18 post-immunization, 6 mice were selected from each group to collect lymph nodes and eyeballs, and the proportion of T cell subsets was detected by flow cytometry. The eyeballs of 6 mice in each group were extracted on day 24 post-immunization and retinal damage was observed by hematoxylin-eosin staining.

1.2.6 EAU Clinical Scoring From day 10 post-immunization, the mice in the anti-IL-12/IL-23 p40 group and the IgG group were subjected to fundus examination using direct ophthalmoscopy after pupil dilation every 1 d. The degree of EAU severity was scored according to the criteria of Caspi: normal fundus scored 0 points; less than 3 central retinal focal damage scored o.5 points; more than 1 but less than 5 peripheral and central retinal focal damage scored 1 points; more than 5 diffuse chorioretinal lesions and less than 5 linear lesions scored 2 points; large confluent retinochoroidal lesions with retinal edema, numerous focal lesions and linear lesions scored 3 points. The presence of extensive retinal detachment was scored as 4 [15].

1.2.7 Flow cytometry detection of CD4$^+$ T cell differentiation *in vitro* CD4 cells were isolated by magnetic bead sorting using a CD4 cell isolation kit. Prior to immunization, the spleen and inguinal lymph node cell suspensions were prepared by grinding followed by an incubation in erythrocyte lysis buffer for 5 min. Next, 20 μL of antibody mixture per 1 × 10^7 cells was added and incubated at 4°C for 20 min before rinsing once with isolation buffer. After washing, 200 μL pre-washed negative magnetic beads were added, shaken gently on a shaker, and incubated at room temperature for 15 min. The tubes were placed on a magnet for 2 min and the collected suspension consisted of CD4$^+$ T cells. Then, 96-well plates were coated with a conjugated anti-mouse CD3 (10 μg/mL) antibody overnight at 4°C. The sorted CD4$^+$ T cells were seeded into the 96-well plate (2 × 10^5 cells per well) and stimulated with soluble CD28 (2.5 μg/mL). The cells were divided into the anti-IL-12/IL-23 p40 group or IgG group, and anti-IL-12/IL-23 p40 (10 ng/mL) or IgG (10 ng/mL) antibodies were added, respectively. Cellular differentiation was induced by the addition of cytokines. Th1: IL-12 (60 ng/mL), anti-IL-4 (300 ng/mL); Th17:

transforming growth factor (TGF)-β (5 ng/mL), IL-6 (10 ng/mL), and IL-23 (10 ng/mL); IL-17A$^+$ IFN-γ$^+$ cells: IL-12 (1 ng/mL), TGF-β (5 ng/mL), IL-23 (10 ng/mL), and IL-6 (10 ng/mL). Next, 200 μL/well cell suspension was added and cultured at 37°C in a 5% CO_2 incubator. After 4 days, the supernatant and cells in each group were collected. Flow cytometry was used to detect the induced differentiation of Th1, Th17, and IL-17A$^+$ IFN-γ$^+$ T cells in the two groups. The remaining supernatant and cells were stored at -80°C until further use.

1.2.8 Enzyme-linked immunosorbent assay An enzyme-linked immunosorbent assay (ELISA) was used to quantitatively detect the concentration of IL-17 and IFN-γ in the anti-IL-12/IL-23 p40 group and IgG group following the differentiation of IL-17A$^+$ IFN-γ$^+$ CD4$^+$ T cells. ELISA kits were used to detect the cell supernatants of the anti-IL-12/IL-23 p40 group and IgG group in accordance with the manufacturer's instructions. The capture antibody was plated on a 96-well plate, incubated at 4°C overnight, and blocked with reagent diluent for 1 h. The cellular supernatant and mouse recombinant IFN-γ standard were added and incubated for 2 h at room temperature. A biotinylated goat anti-mouse IFN-γ antibody was added and incubated for 2 h at room temperature. Next, streptavidin was added and incubated at room temperature for 20 min in the dark before adding chromogenic reagent and incubating at room temperature for a further 20 min. Stop solution was added, and the level of IL-17 and IFN-γ expression in each group was quantitatively detected using a microplate reader at a wavelength of 540 nm or 570 nm.

1.2.9 Real-time fluorescence quantitative PCR To detect the relative expression of transcription factors in Th1 and Th17 cells after inducing cell differentiation, an EZ-press RNA purification kit was used to extract mRNA of cells in the anti-IL-12/IL-23 p40 group and IgG group. The mRNA was reverse transcribed into cDNA using a reverse transcription kit for PCR amplification. Primers were purchased from Tianjin Jinweizhi Biotechnology Co., Ltd. The forward primer sequence of T-bet is 5'-TCACTAAGCAAGGACGGCGAATGTT-3', reverse primer sequence is 5'-GGACATATAAGCGGTTCCCTGGCAT-3'. The forward primer sequence of retinoid-related orphan nuclear receptor γt (ROR-γt) is 5'-ACCTCTTTTCACGGGAGGA-3', the reverse primer sequence is 5'-TCCCACATCTCCCACATTG-3'. The forward primer sequence of glyceraldehyde 3 phosphate dehydrogenase (GAPDH) is 5'-GCACCGTCAAGGCTGAGAAC-3', the reverse primer sequence is 5'-TGGTGAAGACGCCAGTGGA-3'. The following PCR reaction conditions were used: pre-denaturation at 95°C for 30 s, denaturation at 95°C for 30 s, and annealing at 60°C for 30 s for a total of 40 cycles. All data were normalized to GAPDH and the $2^{-\Delta\Delta Ct}$ method was used to calculate the level of relative gene expression. Three samples were analyzed for each group and three replicate wells were plated for each sample.

1.3 Statistical Analysis

Statistical analysis was conducted using SPSS version 23.0 for Windows. The measurement data was confirmed by the Shapiro-Wilk test to be in accordance with the normal distribution, expressed as $x \pm s$. Those that did not conform to the normal distribution were expressed as M (Q1, Q3). Comparison of the percentages of IL-17A$^+$ IFN-γ$^+$ CD4$^+$ T cells at different time points in each tissue using Kruskal-Wallis test. The overall comparison of retinal performance scores at different time points post-immunization between the anti-IL-12/IL-23 p40 group and IgG group was performed using a repeated measures two-way ANOVA, and pairwise comparison was performed by SNK-q test. An independent samples t-test was used to compare the differentiation ratio of Th1, Th17, IL-17A$^+$ IFN-γ$^+$ CD4$^+$ T cells, the expression of IL-17A, IFN-γ, and their transcription factors between the anti-IL-12/IL-23 p40 group and IgG group. Differences with $P < 0.05$ were considered significant.

2 Results

2.1 Comparison of the proportion of IL-17A$^+$ IFN-γ$^+$ CD4$^+$ T cells in the spleen, lymph node and eyeball tissues at different time points before and after immunization in EAU mice

Flow cytometry revealed that the overall differences in the proportion of IL-17A$^+$ IFN-γ$^+$ CD4$^+$ T cells in the lymph nodes, spleen, and eyeballs before immunization and on days 3, 12, and 18 post-immunization were statistically significant (H = 9.642, 16.531, 10.385, both $P < 0.05$). Compared with pre-immunization and day 12 post-immunization, the proportion of IL-17A$^+$ IFN-γ$^+$ CD4$^+$ T cells in the lymph nodes were significantly increased. On day 18 post-immunization, the proportion of IL-17A$^+$ IFN-γ$^+$ CD4$^+$ T cells in the spleen and eyeball were significantly increased (all $P <$ 0.05) (Figure 1, Table 1).

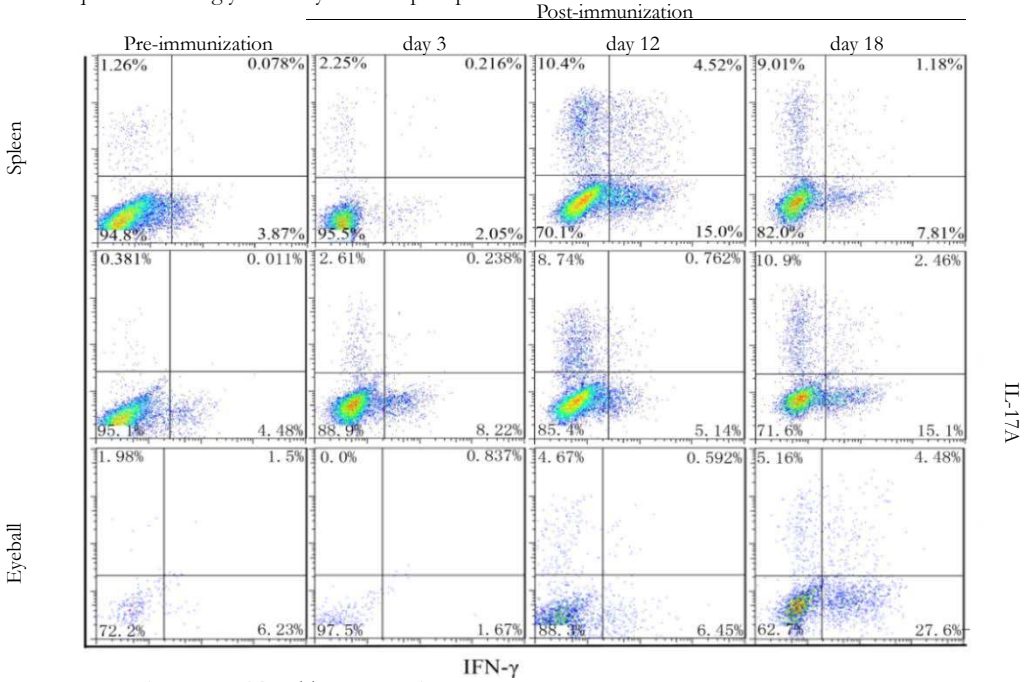

Figure 1 Percentage of IL-17A$^+$ IFN-γ$^+$ CD4$^+$ T cells in EAU mice at different time points before and after immunization detected by flow cytometry. Compared with pre-immunization, the proportion of IL-17A$^+$ IFN-γ$^+$CD4$^+$ T cells was significantly increased in lymph nodes on day 12 post-immunization, and was significantly increased in spleen and eyeball on day 18 post-immunization

Table 1 Comparison of the proportion of IL-17A$^+$ IFN-γ$^+$ CD4$^+$ T cells in different mouse tissues at different time points ($M[Q_1,Q_3]$, %)

Time	Sample size	Proportion of IL-17A$^+$ IFN-γ$^+$ CD4$^+$ T cells in different tissues		
		Lymph node	Spleen	Eyeball
Pre-immunization	6	0.08(0.01,0.11)	0.01(0.01,0.02)	1.63(1.50,1.70)
Day 3 post-immunization	6	0.18(0.05,0.22)	0.13(0.09,0.24)	1.29(0.84,4.03)
Day 12 post-immunization	6	4.53(4.52,4.55)[a]	0.45(0.27,0.76)	0.80(0.59,4.93)
Day 18 post-immunization	6	1.19(0.87,1.27)	1.52(1.28,2.46)[a]	3.15(1.98,4.48)[a]
H		9.462	16.531	10.385
P		0.024	0.001	0.016

Note: Compared with pre-immunization, [a]$P < 0.05$ (Kruskal-Wallis *H* test) IL: interleukin; IFN-γ: interferon-γ

2.2 Comparison of retinal inflammation between IL-17A$^+$ IFN-γ$^+$ high expression group and IL-17A$^+$ IFN-γ$^+$ low expression group

Fundus photography showed large confluent retinal choroid damage, retinal edema, a large number of focal and linear damage in the IL-17A$^+$ IFN-γ$^+$ high expression group. Diffuse chorioretinal damage was observed in the IL-17A$^+$ IFN-γ$^+$ low expression group (Figure 2). The OCT images revealed retinal edema, substantial inflammatory cell leakage, and retinal detachment in the IL-17A$^+$ IFN-γ$^+$ high expression group. Mild retinal edema and a small amount of inflammatory cell leakage was found in the IL-17A$^+$ IFN-γ$^+$ low expression group (Figure 3). The hematoxylin-eosin staining results showed that the IL-17A$^+$ IFN-γ$^+$ high expression group exhibited substantial inflammatory cell infiltration in all retinal layers and vitreous cavity, high retinal folds, large areas of retinal detachment, and unclear boundaries of retinal layers were (Figure 4).

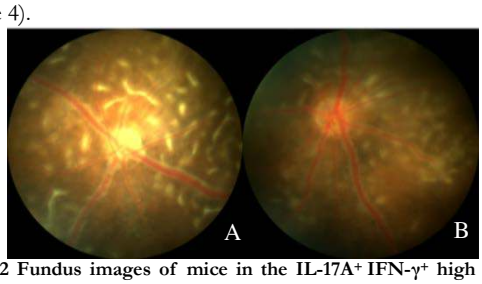

Figure 2 Fundus images of mice in the IL-17A$^+$ IFN-γ$^+$ high expression group and IL-17A$^+$ IFN-γ$^+$ low expression group. A: IL-17A$^+$ IFN-γ$^+$ high expression group Large confluent retinal choroidal injury, retinal edema, and multiple focal and linear injuries were observed B: IL-17A$^+$ IFN-γ$^+$ low expression group Diffuse retinal choroidal injury was observed

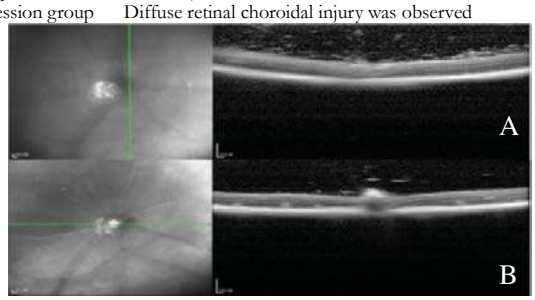

Figure 3 OCT images of fundus in the mice A: IL-17A$^+$ IFN-γ$^+$ high expression group Thickening of retina, leakage of substantial inflammatory cells and retinal detachment were observed B: IL-17A$^+$ IFN-γ$^+$ low expression group Mild retinal edema and a small amount of inflammatory cell leakage was found

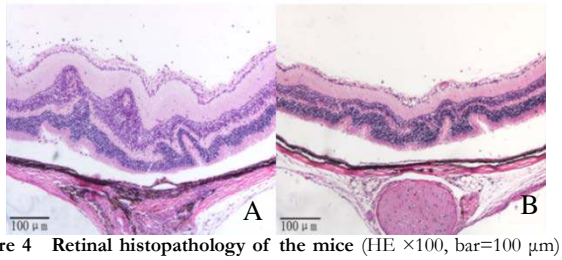

Figure 4 Retinal histopathology of the mice (HE ×100, bar=100 μm) A: IL-17A$^+$ IFN-γ$^+$ high expression group Infiltrating of large number of inflammatory cells in various layer of retina and vitreous cavity, severe retinal folds and retinal detachment were displayed. The interlayer structure of the retina was indistinct B: IL-17A$^+$ IFN-γ$^+$ low expression group A few inflammatory cells in retina and vitreous cavity and moderate retinal folds were seen. The retinal structure was clear

2.3 Comparison of retinal clinical scores and inflammation between IgG group and anti-IL-12/IL-23 p40 group

A significant difference was observed in the overall comparison of retinal clinical scores between the IgG group and the anti-IL-12/IL-23 p40 group at different time points (F_{group}=15.045, P = 0.03; F_{time}=99.764, $P < 0.01$). The retinal clinical scores on days 12, 14, 16, 18, 20, 22, and 24 post-immunization were all significantly lower than those in the IgG group (all $P < 0.01$) (Table 2). Hematoxylin-eosin staining revealed heavy inflammatory cell infiltration and extensive retinal folding with detachment in the IgG group. Moderate inflammatory cell infiltration and retinal folds appeared in each retinal layer in the anti-IL-12/IL-23 p40 group (Figure 5).

Flow cytometry showed that the proportion of CD3$^+$ cells in the eyeball on day 18 post-immunization in the anti-IL-12/IL-23 p40 group was 13.58% ± 4.70%, which was significantly lower than that in the IgG group 90.11% ± 8.07%. The difference was statistically significant (t=15.304; $P < 0.01$). The proportion of IL-17A$^+$ IFN-γ$^+$ CD4$^+$ T cells in the eyeball of the anti-IL-12/IL-23 p40 group was 1.52% ± 0.29%, which was significantly lower than that of the IgG group (4.95% ± 0.68%) (t=8.080, $P < 0.05$). On day 12 post-immunization, the proportion of IL-17A$^+$ IFN-γ$^+$ CD4$^+$ T cells in the lymph nodes of the anti-IL-12/IL-23 p40 group was 0.33% ± 0.18%, which was significantly lower than that of the IgG group (4.83% ± 0.45%) (t=15.974, P<0.001) (Figure 6).

Table 2 Comparison of retinal inflammation scores at different time points after immunization between two groups ($\bar{x}\pm s$, score)

Group	Sample Size	Score of retinal inflammation in different time after immunization							
		10 days	12 days	14 days	16 days	18 days	20 days	22 days	24 days
IgG group	6	0.08±0.20	0.83±0.41	1.67±0.52	2.33±0.41	2.83±0.52	2.67±0.41	2.08±0.38	1.75±0.27
Anti-IL-12/IL-23 p40 group	6	0.00±0.00	0.17±0.26[a]	0.83±0.41[a]	1.67±0.41[a]	2.08±0.38[a]	2.00±0.45[a]	1.50±0.45[a]	1.17±0.41[a]

Note: F_{group}=15.045, P=0.03; F_{time}=99.764, $P < 0.01$. Compared with IgG group at respective time points, [a]$P < 0.01$ (Two-way repeated measures ANOVA, SNK-q test). IL: interleukin

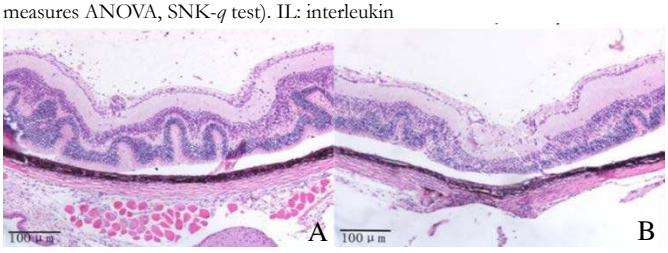

Figure 5 Retinal histopathology of the mice (HE ×100, bar=100 μm) A: IgG group The interlayer structure was indistinct, and a lots of inflammatory cells, extensive retinal folds and retinal detachment were seen B: Anti-IL-12/IL-23 p40 group The inflammatory cell infiltration, retinal folds were lessening in comparison with the IgG group

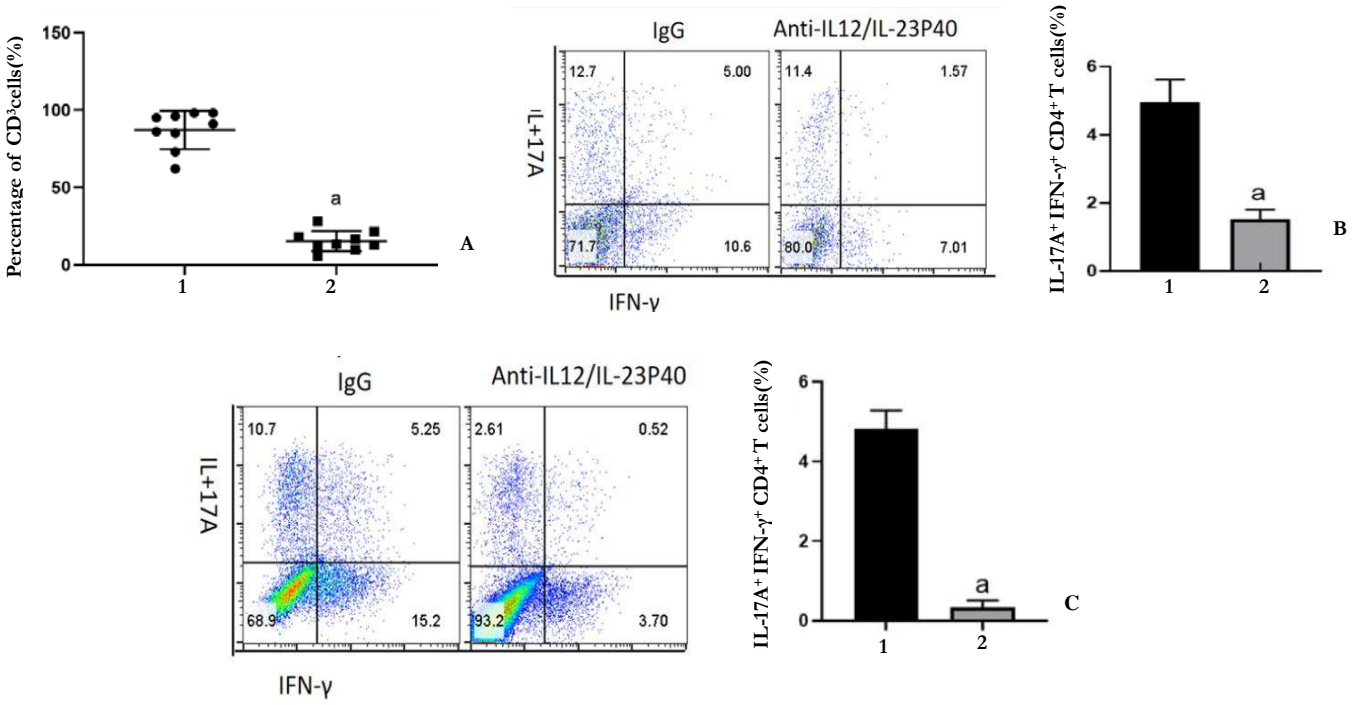

Figure 6 Comparison of the proportion of IL-17A+IFN-γ+CD4+ T cells between IgG group and anti-IL-12/IL-23 p40 group at different time points by flow cytometry A: Comparison of CD3 cells in eyeballs on day 12 after immunization Compared with IgG group, ^aP<0.01 (Independent samples *t* test, *n*=9) B: Comparison of the percentage of IL-17A+ IFN-γ+ CD4+ T cells in eyeballs on day 18 after immunization Compared with IgG group, ^aP<0.05 (Independent sample *t* test, *n*=6) C: Comparison of the proportion of IL-17A+ IFN-γ+ CD4+ T cells in lymph nodes on day 12 after immunization Compared with IgG group, ^aP<0.05 (Independent samples *t* test, *n*=6) IL: interleukin; IFN: interferon 1: IgG group 2: anti-IL-12/IL-23 p40 group

2.4 Comparison of the Th1, Th17, and IL-17A+ IFN-γ+ CD4+ T cell differentiation ratio, IL-17A, IFN-γ and their transcription factor expression between groups

Flow cytometry showed that compared with the IgG group, the percentages of Th1, Th17, and IL-17A+ IFN-γ+ CD4+ T cells in the anti-IL-12/IL-23 p40 group were significantly decreased (*t*=22.876, 0.634, 7.025; all *P* < 0.01 (Table 3). The ELISA results showed that compared with the IgG group, the concentrations of IL-17 and IFN-γ in the anti-IL-12/IL-23 p40 group were significantly lower (*t*=9.580, 46.412; both *P* < 0.001) (Table 4). The results of real-time fluorescence quantitative PCR showed that the relative level of T-bet and ROR-γt mRNA expression in the anti-IL-12/IL-23 p40 group were significantly lower than those in the IgG group (*t*=6.097, 7.526; both *P* < 0.05) (Table 5).

Table 3 Comparison of the percentage of Th1, Th17 and IL-17A+ IFN-γ+ CD4+ T cells between two groups ($\bar{x}\pm s$, %)

Group	Sample size	Th1 cells	Th17 cells	IL-17A+ IFN-γ+CD4+ T cells
IgG group	3	29.80±1.15	21.27±0.91	5.43±0.89
anti-IL-12/IL-23 p40 group	3	13.20±0.49	8.71±0.66	1.67±0.27
t		22.876	0.634	7.025
P		<0.001	<0.001	0.002

Note: (Independent samples *t* test) IL: interleukin; IFN-γ: interferon-γ

Table 4 Comparison of IL-17A and IFN-γ concentration between two groups ($\bar{x}\pm s$, pg/ml)

Group	Sample size	IL-17A	IFN-γ
IgG group	3	47.28±4.77	794.67± 8.08
anti-IL-12/IL-23 p40 group	3	18.08±3.80	399.33±12.34
t		9.580	46.412
P		<0.001	<0.001

Note: (Independent samples *t* test) IL: interleukin; IFN-γ: interferon-γ

Table 5 Comparison of relative expression of T-bet and ROR-γt mRNA between two groups ($\bar{x}\pm s$)

Group	Sample size	T-bet	ROR-γt
IgG group	3	0.0054±0.0019	0.0101±0.0017
anti-IL-12/IL-23 p40 group	3	0.0009±0.0004	0.0013±0.0011
t		6.097	7.526
P		0.040	0.002

Note: (Independent samples *t* test) ROR-γt: retinoid-related orphan nuclear receptor γt

3 Discussion

IL-17A$^+$ IFN-γ$^+$ CD4$^+$ T cells are associated with strong pathogenicity [16]. In both *in vivo* and *in vitro* experiments, IL-17A$^+$ IFN-γ$^+$ CD4$^+$ T cells preferentially cross the human blood-brain barrier. In addition, in the experimental autoimmune encephalomyelitis (EAE) model, IL-17A$^+$ IFN-γ$^+$ CD4$^+$ T cells has been shown to accumulate in the central nervous system during the symptomatic period of EAE [17].

On day 3 post-EAU immunization, our results showed little infiltration of IL-17A$^+$ IFN-γ$^+$ CD4$^+$ T cells in the various tissues. As the disease progressed, IL-17A$^+$ IFN-γ$^+$ CD4$^+$ T cells increased continuously. IL-17A$^+$ IFN-γ$^+$ CD4$^+$ T cells in the draining lymph nodes on day 12 post-immunization increased significantly, whereas IL-17A$^+$ IFN-γ$^+$ CD4$^+$ T cells in the eyeball and spleen peaked on day 18 of EAU immunization. The above results suggest that on day 12 post-immunization, the immune response in the draining lymph nodes was activated, and IL-17A$^+$ IFN-γ$^+$ CD4$^+$ T cells were abundant in the lymph nodes. At the same time, IL-17A$^+$ IFN-γ$^+$ CD4$^+$ T cells in the peripheral immune tissues began to circulate and infiltrate into the spleen and eye-specific inflammatory tissue sites. Therefore, after the 12th day of immunization, as the disease progressed, IL-17A$^+$ IFN-γ$^+$ CD4$^+$ T cells in the lymph nodes decreased, whereas IL-17A$^+$ IFN-γ$^+$ CD4$^+$ T cells in the spleen and eyeball gradually increased. Shuang et al. [18] studied the clinical score of the EAU model and found that inflammation began on the 9th-12th days after modeling, and the peak period of inflammation was on the 16th-18th days after modeling. The present study indicated that IL-17A$^+$ IFN-γ$^+$ CD4$^+$ T cells in the eyeball started to appear at the initial stage of inflammation and peaked during the height of the inflammatory response. In addition, this study found that the pathological sections and retinal images of mice with higher levels of IL-17A$^+$ IFN-γ$^+$ CD4$^+$ T cells in the process of EAU exhibited more severe disease. Therefore, the present study concluded that IL-17A$^+$ IFN-γ$^+$ CD4$^+$ T cells were more abundant, indicating that EAU was more severe. Monoclonal antibodies that share the p40 subunit of IL-12 and IL-23 can inhibit the signal transduction mediated by IL-12R and IL-23R; therefore, the p40 subunit is important for the formation of IL-17A$^+$ IFN-γ$^+$ CD4$^+$ T cells. This study explored the role of IL-12/IL-23 in EAU progression, which was neutralized by inhibiting the differentiation of IL-17A$^+$ IFN-γ$^+$ CD4$^+$ T cells. The results suggest that after the anti-IL-12/IL-23 p40 antibody was injected into the tail vein of EAU mice, the clinical scores and retinal damage in the anti-IL-12/IL-23 p40 group were alleviated, including the level of inflammatory cell infiltration, number of retinal folds, number of chorioretinal neovascularization, and area of retinal detachment, which were all decreased. In addition, the proportion of CD3 cells in the eyeball on day 18 post-immunization was also significantly lower than that of the control group. This study further verified the effect of anti-IL-12/IL-23 p40 on T cell inflammatory factors using *in vitro* experiments. When inducing CD4$^+$ T cell differentiation, compared with the IgG group, the anti-IL-12/IL-23 p40 group could significantly inhibit the differentiation of Th1, Th17, and IL-17A$^+$ IFN-γ$^+$ CD4$^+$ T cells. This finding indicates that anti-IL-12/IL-23 p40 treatment can alleviate the ocular pathology of EAU mice by inhibiting the infiltration of IL-17A$^+$ IFN-γ$^+$ CD4$^+$ T cells, and delay the occurrence of EAU. This study further explored the effects of anti-IL-12/IL-23 p40 against EAU and investigated its potential mechanism. The transcription factors, T-bet and RoR-γt, are unique to Th1 and Th17 cells, respectively. The findings of this study suggest that anti-IL-12/IL-23 p40 can reduce the expression of T-bet and ROR-γt in IL-17A$^+$ IFN-γ$^+$ CD4$^+$ T cells. Therefore, the therapeutic effect of anti-IL-12/IL-23 p40 treatment on EAU may be partially mediated by inhibiting the expression of Th1 and Th17 transcription factors, T-bet and ROR-γt. Furthermore, IL-17A$^+$ IFN-γ$^+$ differentiation of CD4$^+$ T cells may also be inhibited by anti-IL-12/IL-23 p40 treatment. However, the changes in other related genes have not been detected in this study. Further verification will be conducted in our subsequent research.

In an experimental model of inflammatory bowel disease (IBD), the transition of Th17 cells to IL-17A$^+$ IFN-γ$^+$CD4$^+$ T cells requires T-bet and STAT4 expression [2]. In the EAE model, it has been shown that the transcription factors T-bet, Runx1, and Runx3 initiate the differentiation of Th17 cells into IL-17A$^+$ IFN-γ$^+$CD4$^+$ T cells. Chen et al. [19] confirmed that the IL-17A$^+$ IFN-γ$^+$CD4$^+$ T cell population was derived from Th17 precursors and played a pathogenic role in a dry eye mouse model. However, a new has study demonstrated that Th1 cells can transdifferentiate into Th17 cells under the influence of TGF-β and IL-6. In this model, RUNX1 expression was upregulated, the increasing accessibility of the RunX1 binding site in the ROR-γt promoter, as well as the RunX1 and ROR-γt binding sites in the IL-17 promoter [20-22]. Therefore, the route of IL-17A$^+$ IFN-γ$^+$ CD4$^+$ T cell differentiation or whether IL-17A$^+$ IFN-γ$^+$ CD4$^+$ T cells represent a stable CD4$^+$ T cell subset have not been clarified. In this study, although anti-IL-12/IL-23p40 could effectively alleviate the ocular pathological manifestations of EAU, the disease was not completely suppressed, which may be due to the presence of IL-17A$^+$ IFN-γ$^+$CD4$^+$T cells.

The elevation of IL-17A$^+$ IFN-γ$^+$ CD4$^+$ T cells in EAU retinal inflammation may represent a selective target for biologics. In future studies, we hope to induce IL-17A$^+$ IFN-γ$^+$ CD4$^+$ T cells to evaluate their ability to promote disease in adoptive transfer experiments. We believe that targeting the plasticity of IL-17A$^+$ IFN-γ$^+$ CD4$^+$ T cells with biologics will provide a valuable tool for potential future uveitis treatment strategies.

Conflict of interest None declared.

Author contributions Cui Xuexue: topic selection, designing experiments, implementing research, collecting data, analyzing/interpreting data, drafting articles; Zhang Zhihui, Wu Lingzi, Li Yongtao, Chen Shuang, and Chen Nu: topic selection, designing experiments; Zhang Xiaomin: topic selection, review of the intellectual content of the article, revision, and finalization of intellectual content.

References

[1] Wang Y, Godec J, Ben-Aissa K, et al. The transcription factors T-bet and Runx are required for the ontogeny of pathogenic interferon-γ-producing T helper 17 cells[J]. Immunity, 2014, 40(3):355-366. DOI: 10.1016/j.immuni.2014.01.002.

[2] Harbour SN, Maynard CL, Zindl CL, et al. Th17 cells give rise to Th1 cells that are required for the pathogenesis of colitis[J]. Proc Natl Acad Sci U S A, 2015, 112(22):7061-7066. DOI: 10.1073/pnas.1415675112.

[3] van Langelaar J, van der Vuurst de Vries RM, Janssen M, et al. T helper 17.1 cells associate with multiple sclerosis disease activity: perspectives for early intervention[J]. Brain, 2018, 141(5):1334-1349. DOI: 10.1093/brain/awy069.

[4] Srivastava RK, Dar HY, Mishra PK. Immunoporosis: immunology of osteoporosis-role of T cells[J/OL]. Front Immunol, 2018, 9:657[2021-12-05]. https://pubmed.ncbi.nlm.nih.gov/29675022/. DOI: 10.3389/fimmu.2018.00657.

[5] Diedrichs-Möhring M, Kaufmann U, Wildner G. The immunopathogenesis of chronic and relapsing autoimmune uveitis-Lessons from experimental rat models[J]. Prog Retin Eye Res, 2018, 65:107-126. DOI: 10.1016/j.preteyeres.2018.02.003.

[6] Ghoreschi K, Laurence A, Yang XP, et al. Generation of pathogenic T(H)17 cells in the absence of TGF-β signalling[J]. Nature, 2010, 467(7318):967-971. DOI: 10.1038/nature09447.

[7] Volpe E, Servant N, Zollinger R, et al. A critical function for transforming growth factor-beta, interleukin 23 and proinflammatory cytokines in driving and modulating human T(H)-17 responses[J]. Nat Immunol, 2008, 9(6):650-657. DOI: 10.1038/ni.1613.

[8] Okamoto S, Fujiwara H, Nishimori H, et al. Anti-IL-12/23 p40 antibody attenuates experimental chronic graft-versus-host disease via suppression of IFN-γ/IL-17-producing cells[J]. J Immunol, 2015, 194(3):1357-1363. DOI: 10.4049/jimmunol.1400973.

[9] Bastian D, Sui X, Nguyen HD, et al. Interleukin-23 receptor signaling by interleukin-39 potentiates T cell pathogenicity in acute graft-versus-host disease[J]. Am J Transplant, 2021, 21(11):3538-3549. DOI: 10.1111/ajt.16624.

[10] Leonardi CL, Kimball AB, Papp KA, et al. Efficacy and safety of ustekinumab, a human interleukin-12/23 monoclonal antibody, in patients with psoriasis: 76-week results from a randomised, double-blind, placebo-controlled trial (PHOENIX 1)[J]. Lancet, 2008, 371(9625):1665-1674. DOI: 10.1016/S0140-6736(08)60725-4.

[11] Papp KA, Langley RG, Lebwohl M, et al. Efficacy and safety of ustekinumab, a human interleukin-12/23 monoclonal antibody, in patients with psoriasis: 52-week results from a randomised, double-blind, placebo-controlled trial (PHOENIX 2)[J]. Lancet, 2008, 371(9625):1675-1684. DOI: 10.1016/S0140-6736(08)60726-6.

[12] McInnes IB, Kavanaugh A, Gottlieb AB, et al. Efficacy and safety of ustekinumab in patients with active psoriatic arthritis: 1 year results of the phase 3, multicentre, double-blind, placebo-controlled PSUMMIT 1 trial[J]. Lancet, 2013, 382(9894):780-789. DOI: 10.1016/S0140-6736(13)60594-2.

[13] Sandborn WJ, Gasink C, Gao LL, et al. Ustekinumab induction and maintenance therapy in refractory Crohn's disease[J]. N Engl J Med, 2012, 367(16):1519-1528. DOI: 10.1056/NEJMoa1203572.

[14] Wang BB, Tian QM, Xie XF, et al. Dynamic expression and mechanism of γδ T cells in the spleen of mouse with experimental autoimmune uveitis[J]. Chin J Exp Ophthalmol, 2017, 35(9):793-798. DOI: 10.3760/cma.j.issn.2095-0160.2017.09.006.

[15] Agarwal RK, Silver PB, Caspi RR. Rodent models of experimental autoimmune uveitis[J]. Methods Mol Biol, 2012, 900:443-469. DOI: 10.1007/978-1-60761-720-4_22.

[16] Gartlan KH, Varelias A, Koyama M, et al. Th17 plasticity and transition toward a pathogenic cytokine signature are regulated by cyclosporine after allogeneic SCT[J]. Blood Adv, 2017, 1(6):341-351. DOI: 10.1182/bloodadvances.2016002980.

[17] Kebir H, Ifergan I, Alvarez JI, et al. Preferential recruitment of interferon-gamma-expressing TH17 cells in multiple sclerosis[J]. Ann Neurol, 2009, 66(3):390-402. DOI: 10.1002/ana.21748.

[18] Chen S, Shao XF, Zhang ZH, et al. Differential expression and bioinformatics analysis of retinal proteins in mice with experimental autoimmune uveitis[J]. Chin J Exp Ophthalmol, 2019, 37(12):949-955. DOI: 10.3760/cma.j.issn.2095-0160.2019.12.003.

[19] Chen Y, Chauhan SK, Shao C, et al. IFN-γ-expressing Th17 cells are required for development of severe ocular surface autoimmunity[J]. J Immunol, 2017, 199(3):1163-1169. DOI: 10.4049/jimmunol.1602144.

[20] Leipe J, Pirronello F, Klose A, et al. Increased plasticity of non-classic Th1 cells toward the Th17 phenotype[J]. Mod Rheumatol, 2020, 30(5):930-936. DOI: 10.1080/14397595.2019.1667473.

[21] Geginat J, Paroni M, Kastirr I, et al. Reverse plasticity: TGF-β and IL-6 induce Th1-to-Th17-cell transdifferentiation in the gut[J]. Eur J Immunol, 2016, 46(10):2306-2310. DOI: 10.1002/eji.201646618.

[22] Liu HP, Cao AT, Feng T, et al. TGF-β converts Th1 cells into Th17 cells through stimulation of Runx1 expression[J]. Eur J Immunol, 2015, 45(4):1010-1018. DOI: 10.1002/eji.201444726.